Analysis of Combined Convective and Film Cooling on an Existing Turbine Blade

Wim B. de Wolf
National Aerospace Laboratory
P.O. Box 153
8300 AD Emmeloord
The Netherlands

Sandor Woldendorp and Tiedo Tinga
National Aerospace Laboratory
P.O. Box 90502
1006 DM Amsterdam
The Netherlands

Summary

To support gas turbine operators, NLR is developing capabilities for life assessment of hot engine components. As a typical example the first rotor blades of the high pressure (HP) turbine of the F-100-PW-220 military turbofan will be discussed. For these blades tools have been developed to derive the blade temperature history from flight data obtained from F-16 missions. The resulting relative life consumption estimate should support the Royal Netherlands Air Force in their engine maintenance activities.

The present paper describes the prediction method for the blade temperature, based on reverse engineering. Input data are the flight data of the engine performance parameters and the geometry of the HP turbine blades and vanes including film cooling orifices. The engine performance parameters are converted in HP turbine entry and exit conditions by the NLR Gas Turbine Simulation Program (GSP) engine model. Next a Computational Fluid dynamics (CFD) tool is used to calculate the resulting flow field and heat transfer coefficients without film cooling. An engineering method is used to predict the internal cooling and the resulting film injection temperature. The film cooling efficiency is estimated and a finite element method (FEM) for heat conduction completes the analysis tool. The method is illustrated by results obtained for the engine design point.

1. Introduction

Gas turbine operators increasingly recognise that the actual lives of gas turbine hot section components often do not reach the predictions. Consequently, there is a greater demand for residual life assessments incorporating operational gas turbine parameters and conditions. To respond to this demand, the National Aerospace Laboratory NLR of the Netherlands has developed activities and capabilities to assess lives of gas turbine components.

To develop a life prediction model five main disciplines have to be integrated (see Fig.1). These disciplines are applied as follows for a turbine blade:

- Engine System Performance Analysis, to determine the operational conditions of the turbine (entry pressure, temperature, mass flow, rpm) from engine performance history data.
- Fluid Dynamic Analysis, to determine the thermal and mechanical loads on a turbine blade depending on the operational conditions of the turbine.
- Thermal Analysis, to calculate the temperature distribution in the blade material.
- Stress Analysis, to calculate the thermal and mechanical stresses in the blade material.
- Life Consumption Assessment, in particular by fatigue, creep and oxidation.

The analysis tool developed by NLR enables gas turbine operators to optimise their inspection intervals, maintenance planning, component replacement and consequently their costs.

To develop an integrated engine design tool with the disciplines involved would require a massive effort that would by far exceed the resources at NLR. An analysis tool can however be based upon reverse engineering using experience with existing engines. The present paper will illustrate such an approach taking the film cooled

Paper presented at the RTO AVT Symposium on "Advanced Flow Management: Part B – Heat Transfer and Cooling in Propulsion and Power Systems", held in Loen, Norway, 7-11 May 2001, and published in RTO-MP-069(I).

Report Documentation Page

Form Approved
OMB No. 0704-0188

1. REPORT DATE	2. REPORT TYPE	3. DATES COVERED
00 MAR 2003	**N/A**	**-**

4. TITLE AND SUBTITLE	5a. CONTRACT NUMBER
Analysis of Combined Convective and Film Cooling on an Existing Turbine Blade	5b. GRANT NUMBER
	5c. PROGRAM ELEMENT NUMBER
6. AUTHOR(S)	5d. PROJECT NUMBER
	5e. TASK NUMBER
	5f. WORK UNIT NUMBER
7. PERFORMING ORGANIZATION NAME(S) AND ADDRESS(ES) **NATO Research and Technology Organisation BP 25, 7 Rue Ancelle, F-92201 Neuilly-Sue-Seine Cedex, France**	8. PERFORMING ORGANIZATION REPORT NUMBER
9. SPONSORING/MONITORING AGENCY NAME(S) AND ADDRESS(ES)	10. SPONSOR/MONITOR'S ACRONYM(S)
	11. SPONSOR/MONITOR'S REPORT NUMBER(S)

12. DISTRIBUTION/AVAILABILITY STATEMENT
Approved for public release, distribution unlimited

13. SUPPLEMENTARY NOTES
Also see ADM001490, presented at RTO Applied Vehicle Technology Panel (AVT)Symposium held in Leon, Norway on 7-11 May 2001, The original document contains color images.

14. ABSTRACT

15. SUBJECT TERMS

16. SECURITY CLASSIFICATION OF:			17. LIMITATION OF ABSTRACT	18. NUMBER OF PAGES	19a. NAME OF RESPONSIBLE PERSON
a. REPORT	b. ABSTRACT	c. THIS PAGE			
unclassified	**unclassified**	**unclassified**	**UU**	**18**	

Standard Form 298 (Rev. 8-98)
Prescribed by ANSI Std Z39-18

rotor blades of the high-pressure turbine of the Pratt and Whitney F100-PW-220 military turbofan engine as an example. This engine is used by the Royal Netherlands Air Force in their F-16 fighter aircraft.

The variation of the low-pressure turbine entry temperature (FTIT) measured during a typical F-16 mission is shown in figure 2. At take-off FTIT increases from 450 °C (taxi) to 960 °C at full power. At the cruise altitude between 37 and 45 kft FTIT varies between 680 °C and 940 °C. During the descent strong temperature variations occur as a result of frequent changes in power setting.

The present paper will discuss a method to relate the engine operational conditions to the blade temperature of the first stage rotor of the high pressure turbine. The method combines the results from available software tools to predict the engine thermodynamic performance (the NLR Gas Turbine Simulation Program GSP) and the blade aerodynamics (Numeca's FINE/Turbo CFD code available at NLR) with engineering estimates of the internal heat transfer and the film cooling efficiency.

The results may be used to address a number of questions such as: what is the blade failure mode (by creep or fatigue or a combination) and what parts of the mission (and what corresponding power variations) are most life consuming? Finally, a relative or even absolute life consumption estimate can be established to support the engine maintenance activities.

Thermal analysis, stress analysis and the resulting life assessment will not be addressed here but in a future RTO paper.

2. Approach to predict the blade material temperature

The only information available is the blade geometry and the history of the turbine entry and exit conditions. These conditions are available from recorded flight data, combined with a thermodynamic model of the engine to be discussed later. From this information a realistic estimate should be made of the blade temperature and stress history.

The heat transfer calculations are complicated by the fact that the blades are film cooled by high pressure air from the compressor bleed. This air is heated inside the blade before being ejected at a temperature T_{inj} through cooling orifices into the outer flow to provide a cooling air layer with effective temperature T_{film} between the blade surface with temperature $T_{w,ext}$ and the outer hot gas flow.

The external heat transfer q_{ext} (W/m^2) in the case of film cooling can be expressed as (Ref.1):

$$q_{ext} = h_{ext} (T_{film} - T_{w,ext})$$

It is a well accepted engineering approach to assume that the value of the heat transfer coefficient h_{ext} is not affected by the presence of blade film cooling (Ref.1). In that case h_{ext} values can be calculated by well established CFD methods for zero film cooling.

As a result of the discrete point injection and the mixing with the outer flow T_{film} is somewhere between the adiabatic wall temperature without film cooling and T_{inj}. This is expressed by the film cooling efficiency:

$$\eta_{film} = \frac{T_{gas} - T_{film}}{T_{gas} - T_{inj}}$$

Here T_{gas} is the adiabatic wall temperature without film cooling or, in the case of multiple orifice rows $T_{gas} = T_{film}$ just upstream of the orifice row (Ref.2). Orifice diameters on the blades considered here are of the order of 0.3 mm and orifice rows are typically 6 mm apart. The film cooling efficiency will depend on the streamwise distance behind the orifice row and on the lateral (spanwise) distance (Ref.1). As a first simplification, a lateral average may be used. Typical values are of the order of 0.2 close to the orifice row decreasing to 0.1 at 50 orifice diameters downstream (see for instance Ref.1, 3).

A further simplification is to replace the orifice row by a narrow slot of width w with the same cooling air mass flow. FINE/Turbo was recently extended with such a slot film cooling model but during its application a number of practical problems were encountered:

- The cooling slots have a width equal to the local grid cell length that was about 5 percent of the blade chord in the mid-chord region. Film temperatures tend to decrease 2 grid cells ahead of the slot due to numerical

diffusion. Smaller grids are required for sufficient resolution but have not been used to avoid unacceptable long computation times.
- The slot cooling model will provide cooling efficiencies that are significantly higher than for orifice cooling near to the orifice rows. This could be compensated for by choosing a higher injection temperature than for the orifice cooling.

FINE/Turbo was therefore used to calculate h_{ext} without film cooling to be used for the calculations with film cooling. The option of slot film cooling was used only to improve the prediction of the pressure distribution.

To calculate the external heat transfer, also the film temperature must be determined. This requires a realistic estimate of the film cooling efficiency. In combination with a prediction for the internal heat transfer the blade temperature distribution can be calculated in an iterative procedure with a Finite Element Method (FEM) model of the blade, starting with an assumed blade temperature distribution. It is noted that the injection temperature follows from the internal heat transfer to the cooling air but in turn the injection temperature affects the film temperature and hence the external heat transfer and thus the blade temperature and thus the heating of the cooling air etc., resulting in an iterative procedure.

For the internal cooling an engineering model based on fully developed pipe flow has been used taking into account the effect of turbulators that increase friction losses and heat transfer. Some of the cooling ducts have orifices that provide the external film cooling. Pressure losses and heat transfer in the orifices can be taken into account again by an engineering prediction.

For calculation of the temperature and the heat conduction in the blade material the computer programs MARC or B2000 are available based on finite element methods.

Figure 3 summarises the approach that will be used, depicting the data flow logic. Data processors are indicated in rectangles. Here ‘e.m.’ stands for engineering methods that are well established and ‘e.e.’ for engineering estimates. These estimates constitute the weakest elements in the method and should be varied in a sensitivity analysis. The estimates relate to (i) the influence of the turbulators and centrifugal forces on internal heat transfer in the serpentine cooling ducts and (ii) to the film cooling efficiency. The next chapters will discuss this approach and some results in more detail.

3. From flight data to turbine entry and exit conditions.

For assessment of the blade life, the blade temperature history and the resulting stresses must be known. The engine operational data obtained during a particular flight mission form the starting point.

F-16 fighter aircraft of the RNLAF are being equipped with a fatigue analysis system developed by NLR, combined with the Autonomous Combat Evaluation (ACE) system to form the FACE system. Presently more than 100 aircraft have an operational FACE system. The relevant signals stored by the FACE Data Recording Unit are engine parameters from the Digital Electronic Engine Control (DEEC) and avionics data. The following relevant data are stored: fuel flow to the core engine, fuel flow to the afterburner, exhaust nozzle position (area) and for the flight conditions: Mach, pressure altitude and air temperature. The DEEC signals can be sampled at a maximum frequency of 4 Hz.

These data are used as input data for the Gas Turbine Simulation Program (GSP). This is a tool for gas turbine performance analysis, developed at NLR (Ref.4). This program enables both steady state and transient simulations for any kind of gas turbine configuration. The simulation is based on one-dimensional modelling of the processes in the various gas turbine components with thermodynamic relations and steady-state characteristics (component maps). For the F100-PW-220 engine the component maps are based on information from the manufacturer, literature data, and test bench data using reverse engineering. Real gas effects are included as well as thermal and mechanical inertia that are important to accurately describe the engine transients.

For the current application, GSP is used to calculate the high-pressure turbine entry (station 4) and exit (station 45) total temperature, total pressure and mass flows including the cooling air supplied to the HP turbine. The fuel flows and nozzle position input data are replaced by the Power Lever Angle (PLA) signal, as obtained from FACE. GSP contains a model of the F100-PW-220 engine control unit, which translates the PLA to the appropriate fuel flows and nozzle area. With the engine geometry data also the flow velocities at station 4 and 45 can be calculated, assuming a uniform pressure and temperature.

For the high pressure turbine at the engine design point the following data are given below as obtained from GSP. The design point corresponds to military thrust at static sea level ISA conditions.

	HP turbine entry (4)	HP turbine exit (45)	
Total pressure p_t	21.369	5.957	bar
Total temperature T_t	1674.7	1193.3	K
Mass flow	45.274	54.836	kg/s
Shaft speed N_2	12910		rpm
Flow area	0.09273	0.13331	m^2
Axial velocity	111.0	255.0	m/s
Axial Mach number	0.142	0.384	-
Static pressure	21.096	5.414	bar

The exit mass flow is 21 percent higher than the entry mass flow as a result of cooling air injection. This cooling air is obtained from compressor bleed. At the design point the compressor delivery conditions are p_{t3} = 22.60 bar and T_{t3} = 821 K. Axial flow velocities and Mach numbers are based on the given flow areas. Immediately before the inlet guide vanes (IGV's) the flow area is slightly smaller. It is assumed that the flow at stations 4 and 45 has no tangential velocity component.

4. Operational points in the flight envelope

For the present application, the life consumption of the HP turbine first stage rotor blade is to be determined during a series of flight missions. In this frame work (see figure 1) CFD calculations must be performed to calculate the external flow conditions and the resulting heat transfer coefficients on this rotor blade, using the GSP data as input.

To limit the computational effort, the CFD calculations are performed for a small number of operational points in the flight envelope. Results for other operational points are to be found by means of interpolation.

The following three independent parameters were considered as a result of a dimensional analysis: the corrected rotor speed $N_{2,corr} = N_2 / \sqrt{\theta}$ with $\theta = T_{t4}/T_{ref}$, a Reynolds number / Mach number index $Re/M = p_{t4}/(\mu_{t4}\sqrt{T_{t4}})$ and the turbine pressure ratio. These parameters were compared to their values at the engine design point values. The viscosity μ was calculated by the Sutherland equation. The corrected rotor speed is in fact proportional to the circumferential Mach number. For a constant turbine pressure ratio the axial flow Mach number does not change much with $N_{2,corr}$. As a result the Mach number distribution on the blades will be very similar for given $N_{2,corr}$ and turbine pressure ratio and M can be taken proportional to $N_{2,corr}$

The operational points that occurred for a number of flights have been plotted in the three-dimensional parameter space. In the resulting volume a reference point was selected to which six other points were added to be used for a tri-linear interpolation. In the next table the parameters for the seven operational points for the CFD calculations are given relative to the engine design point.

Operational point	$N_{2,corr}$	Re/M index	PR_{HPT}
Design point	1	1	1
Reference point	1.005	1.342	1.195
N2C –	0.804	1.342	1.195
N2C +	1.155	1.342	1.195
Re/M –	1.005	0.783	1.195
Re/M – –	1.005	0.391	1.195
PR –	1.005	1.342	1.049
PR – –	1.005	1.342	0.747

The heat transfer coefficients are calculated in terms of (dimensionless) Stanton numbers

$$St = \frac{h_{ext}}{\rho \; u \; c_p}$$

Each point in the three-dimensional parameter space corresponds to a single value of the Mach number distribution in the turbine. For the present application the product of density and speed of sound at the turbine entry stagnation conditions as defined by (p_{t4}, T_{t4}) are conveniently used as value for ρu, resulting into

$$\tilde{St} = \frac{h_{ext}}{p_{t4}\sqrt{(c_p / T_{t4})}}$$

5. The cooling air mass flow distribution in the high-pressure turbine

To predict the effect of mass flow addition by cooling air in the turbine, the distribution of the cooling air in the various stages must be determined, the total amount being given by GSP.

Figure 4 shows the computational grid of the stator and rotor blade sections of the high-pressure turbine near the mid-span radius (r = 0.28 m). This grid is used for the CFD calculations. The tapered inlet guide vanes have a chord length of 49 mm. The first stage rotor blades are about 46 mm long and have a nearly constant chord of 35 mm. As shown in figure 5, the IGV's and the rotor blades of the first stage have an extensive coverage of film cooling orifices, in particular near the leading edge, the full pressure side and the forward part of the suction side. To enhance the film coverage, the orifices near the leading edge are oriented towards the spanwise direction. The second stage vanes and blades have no film cooling but only internal air cooling. Except for the second stage rotor blades, the trailing edges are cooled by air blown from slots at the pressure side a few mm upstream of the trailing edge.

The cooling air distribution was estimated by measuring and counting the film cooling orifices on sample vanes and blades. Orifice diameters varied between 0.25 and 0.4 mm. Measurement accuracy was 0.05 mm. The effective orifice area was taken as 80 percent of the geometric area which is a realistic value for pressure ratios $p_{t,cool}/p_{ext} \approx 2$ (choked orifice flow) with external cross flow (Ref.5). Considering the external pressures on the various blades and vanes, an average orifice flow Mach number 0.4 was chosen for the inlet guide vanes, 0.6 for the first stage rotor blades and for the other blades sonic orifice flow was assumed. Average total pressures and temperatures just upstream of the orifices had to be estimated, taking into account internal pressure losses and heat transfer. The result is shown in the next table, using $\gamma = 4/3$ for the specific heat ratio.

	eff orif area per blade	number of blades	total eff orif area	$p_{t,cool}$	$T_{t,cool}$	M_{inj}	Cooling Mass Flow	perc mass flow
	mm^2		mm^2	bar	K		kg/s	%
IGV	63.4	44	2790	21.6	1000	0.4	4.79	49.5
1st R	13.6	68	924	19.2	900	0.6	2.00	20.7
2nd V	16.0	58	928	20	900	1	2.49	25.8
2nd R	2.5	72	146	20	900	1	0.39	4.0
all vanes and blades							9.67	100
all vanes and blades according to GSP							9.57	

In view of the accuracy of the orifice dimensions and the assumptions made, the close agreement with the cooling air mass flow provided by GSP is somewhat fortuitous. At off-design conditions the GSP cooling air mass flows can be used while maintaining the percentage mass flow distribution as shown in the last column.

6. Description of the first stage rotor blade cooling.

Details of the cooling air ducts in first stage rotor blades are shown in figures 6. In fact two cooling air circuits exist with a common supply at the blade root. The front circuit serves the cooling of the forward 20 percent of the blade. The cooling air enters duct 2, separated from the front duct 1 by a perforated wall. Duct 1 contains five orifice rows (b – f) that provide film cooling to the leading edge. The air jets from the perforations in the wall between duct 1 and 2 provide a mix of internal impingement cooling and enhancement of the turbulence level and therewith the heat transfer in duct 1. Orifice rows c-e provide showerhead film cooling of the blade leading edge near the stagnation point with spanwise orientation rather than streamwise orientation of the orifices to improve film coverage.

The rear cooling circuit starts with duct 7 from where part of the cooling air is passing to parallel ducts 8 and 9. Ducts 7 and 8 have each a row of cooling orifices i and j respectively) and cooling air in duct 9 passes through a slot (k) slightly ahead of the trailing edge to cool the trailing edge at the pressure side. Between ducts 7, 8 and 9 the turbulence level is enhanced by the openings between these ducts resembling a pin cooling configuration.

The remaining cooling air at the end of duct 7 near the blade tip returns its direction and passes the serpentine cooling ducts 6 - 3 where duct 5 has a row of cooling orifices at the pressure side of the airfoil (row h) and duct 3 has a row of orifices at the pressure side (row g) as well at the suction side (row a). The serpentine cooling duct walls have small strips at 2.5 mm intervals perpendicular to the flow that increase the turbulence level and as a result the internal heat transfer.

Each of these cooling principles has been studied and described in detail in the literature and their performance could in principle be calculated by extensive CFD calculations. This was not considered a viable approach since grid sizes of the order of say 0.1 mm would be required to model the flow near the cooling orifices. Also the internal cooling in the serpentine cooling ducts subjected to strong Coriolis forces and turbulators is difficult to model. For these aspects engineering predictions are applied instead.

7. Aerodynamic calculations

Aerodynamic calculations of the flow conditions in the high pressure turbine have been performed with the FINE/Turbo code (Ref.6). This CFD model solves the Reynolds-averaged Navier-Stokes equations, complemented with a classical algebraic turbulence model (Baldwin-Lomax). Between the blade rows the 'exit' flow conditions are circumferentially averaged to be used as 'entry' conditions for the next blade row after changing from a rotating to a non-rotating system of axes or vice versa. Film cooling is implemented in the form of slot cooling where the cooling orifices are replaced by narrow slots that run in spanwise direction. Cooling air mass flows are duplicated. The slot width w_{inj} is chosen equal to the local grid cell length.

Using the computational grid as shown in figure 4 with approximately 621,000 grid nodes, calculations were made on the complete turbine with respect to aerodynamics and on the first stage rotor blade also on heat transfer (see section 8) on a limited number of operational points. Each operational point required about 16 hours of computation time using a single processor 'SGI Octane' work station.

Figure 7 shows the resulting Mach numbers near the engine design point (in fact at the reference point at PR_{HPT} = 4.00, see section 4) near to the mid-span radius. Mach numbers are relative to the stator or rotor blade). The results given are without and with film cooling air. In both cases the shaft speed, the mass flow and the flow stagnation pressure and temperature at the turbine entry as well as the static pressure at the turbine exit are the same. The results with film cooling show that the turbine is near to the choked condition, determined by the flow area between the rotor blades of the second stage. The mass added by the film cooling reduces the local flow Mach numbers in the first turbine stage and increases the local flow Mach numbers between the second stage rotor blades. The turbine <u>total</u> pressure ratio is 3.60. This is near to the GSP value 3.59 at the design point.

The Mach number distribution outside the boundary layer on the first stage rotor blades with film cooling at the engine reference point is given in figure 8 as derived from figure 7. The Mach distribution is along the axial coordinate (see also figure 6) with z″ =1 corresponding to 0.0279 m. The location of the orifice rows 'a' .. 'k' is indicated, see also figure 6. The Mach distribution without film cooling is shown as dotted line. Especially near the leading edge considerable differences are predicted. On the suction side the Mach number is reduced by the addition of cooling air up to the suction peak at z'' = 0.75.

8. Calculation of the external heat transfer coefficients

FINE/Turbo is used to calculate the heat transfer coefficient h_{ext} without film cooling. In that case the local Mach numbers are slightly different compared to the situation with film cooling. A fully turbulent boundary layer was assumed. The rotor blade exit Reynolds numbers based on a chord length of 36 mm are 1.2×10^6. At turbulence levels of 10% to be expected in jet engine turbines, the boundary layer will then be turbulent for most of the wetted blade area. Also the presence of the jets from the film cooling orifices will promote turbulence. The assumption of a fully turbulent boundary layer will therefore be realistic and possibly somewhat conservative near the leading edge of the blade.

Figure 9 shows the Stanton number $\tilde{St}$ distribution (defined at end of section 4) on the mid-span radius for the reference condition as a function of the distance s from the stagnation point measured along the blade surface. This stagnation point is assumed to be between orifice rows 'c' and 'd'. The three non-dimensional engine operation parameters at this condition are realised for p_{t4} = 2 MPa, T_{t4} = 1200 K, N_2 = 12500 rpm and p_{45} = 0.5 MPa.

For the situation <u>without</u> film cooling the resulting heat transfer coefficients h_{ext} are obtained through multiplication of $\tilde{St}$ by $p_{t4}\sqrt{(c_p / T_{t4})}$ with p and T in Pa and K respectively. For the situation <u>with</u> film cooling a lower value for the total temperature must be used than the turbine entry value T_{t4} and h_{ext} will be accordingly higher. In fact a correction is made for the higher ρu value at the rotor blade. The procedure will be illustrated below for the engine design point.

At the engine design point p_{t4} = 2.137 MPa and T_{t4} = 1675 K. Cooling air is entering the turbine inlet guide vanes at 821 K. During its passage through the IGV's the air is heated up by the heat flowing from the external blade surface to the cooling ducts. This heat is returning into the external flow by the film cooling air. It follows from the resulting heat balance that the total temperature behind the IGV's must be calculated as a result of mixing 45.3 kg combustion gas at 1675 K with 4.79 kg cooling air of 821 K. The result is a total temperature of 1596 K in the stator frame of reference at the interface between the IGV's and the rotor. It is assumed that the stagnation pressure remains unchanged and equal to 21.37 bar.

The result is that T_{t4} = 1596 K and p_{t4} = 2.137 MPa must be used to calculate h from $\tilde{St}$ as presented in figure 10 for the engine design point. For $\tilde{St}$ = 0.001 a heat transfer coefficient h_{ext} = 1.88 kW/m^2/K results.

CFD calculations predict a (rotor) relative Mach number 0.270 at the mid-span radius at the entry of the rotor computational domain. This results in T_t = 1509 K and p_t = 16.75 bar in the rotor frame of reference at the mid-span radius r = 0.285 m. This temperature can be used as T_{gas} for the calculation of the film temperature for given η_{film} , see section 2.

9. Internal heat transfer and pressure losses

The cooling air flow will be heated on its way through the cooling duct and at the same time its total pressure will reduce as a result of wall friction. Data from Ref.7 were used to estimate of the effect of the turbulators. It is assumed that for the present turbulator configuration the Stanton number St is increased by a factor 2 and $St/(c_f)^{1/3}$ by a factor 1.2 compared to the value of a turbulent fully developed pipe flow. So, c_f increases by a factor 4.6.

Take for example a serpentine cooling duct with a flow Mach number 0.18 with $\rho u \approx 700$ (kg/s)/m^2. Its cross section is of 1.5×5 mm leading to a hydraulic diameter of 2.3 mm. Its length is 46 mm. The cooling air mass flow is 5.2 g/s at T = 1000 K, p = 18 bar and the Reynolds number $Re_{d,hyd}$ is 39 000. This leads to a heat transfer coefficient of 6 kW/m^2/K. For a temperature difference of 100 K between the cooling air and the duct wall the cooling air temperature will increase 56 K in one duct length. Along this duct the total pressure decreases by 4.4 percent. These calculations can be improved in further iteration steps.

Orifice flow pressure losses are estimated at 1.3 percent per diameter length with a turbulent pipe flow model. The orifice heat transfer coefficient is estimated at 10 kW/m^2/K. Taking $\rho u \approx 2200$ (kg/s)/m^2 (sonic flow, discharge coefficient 0.8), an orifice diameter of 0.25 mm and an orifice length of 10 diameters, the cooling air temperature is increased by 16 K across the orifice for 100 K temperature difference between the orifice wall and the cooling air.

10. Coupled heat transfer calculations

10.1 Simple geometry model

For prediction of the temperature distribution in the rotor blade material an iterative calculation procedure is required as described in section 2. Before performing these calculations on the actual rotor blade a computation was made on the simple configuration shown in figure 10, in fact representing the serpentine cooling ducts running along the full blade length of 46 mm.

The side A-B represents part of the blade suction side and C-D part of the pressure side. Cooling air enters duct 6 at a total pressure and temperature of 19.6 bar and 875 K (602 °C). In duct 5 part of the cooling air is ejected through a row of orifices 'h' with a total geometric area of 0.75 mm^2. In duct 3 the remaining cooling air is ejected through orifices 'a' with a total geometric area of 3.0 mm^2 and 'g' with a total geometric area of 0.8 mm^2. External total pressure and temperature are 16.75 bar and 1509 K. At the suction side A-B the local external flow Mach number is 0.6 and at the pressure side C-D this is 0.25. The external heat transfer coefficient is 2.6 kW/m^2/K at the suction side A-B and 2 kW/m^2/K at the pressure side C-D. This corresponds to $\tilde{St}$ = 0.0138 and 0.0106 (see figure 9). The internal heat transfer coefficient in the serpentine ducts is 7 kW/m^2/K. This is slightly higher than the value mentioned in section 9. Orifice heat transfer is neglected. Some compensation is found by taking the injection temperature for the full row equal to the local total temperature in the end of the cooling duct (i.e. at the last orifice). The heat conductivity of the blade material is λ = 20 W/m/K.

10.2 Estimate of cooling air mass flows

The first step is to estimate the cooling air mass flow in the serpentine ducts. This is done by an iterative procedure starting with an assumed total pressure halfway duct 3 that must be higher than the external pressure of 16.09 bar at 'g'. Using a pressure ratio dependent discharge coefficient obtained from Ref.5, the orifice mass flow is determined assuming a total temperature of 1050 K in duct 3. The mass flow in duct 4 is known and the pressure drop due to friction (4.6 times the value in a smooth pipe) can be calculated. Assumed average cooling air temperatures in ducts 4, 5 and 6 are 1000, 950 and 900 K. After including the mass flow from orifice row 'h' the pressure at the entry of duct 6 is calculated and compared to the target value of 19.6 bar. After iteration the following results are found (using air with a specific heat ratio $\gamma = 4/3$ internally and 1.3 externally). Mach numbers and velocities u are in the ducts (4 and 6) or in the jets from the cooling orifices (a, g and h).

		p_t	p_{ext}	C_D	mass flow	Mach	u
		bar	bar		g./s		m/s
orifice row	A	17.20	13.34	0.70	4.05	0.636	390
orifice row	G	17.20	16.09	0.69	0.60	0.318	200
duct (mid)	4	17.84	-	-	4.65	0.160	98.9
orifice row	H	18.48	16.09	0.72	0.90	0.460	273
duct entry	6	19.65	-	-	5.55	0.172	100.8

These mass flows are used in the calculation of the blade temperature distribution and the actual cooling air temperature in the serpentine ducts using the FEM model for the heat conduction inside the blade material.

10.3 Orifice versus slot cooling

Two cases are considered. One is the case with orifice film cooling with an assumed efficiency of 0.15. The other case is with slot cooling, starting with an efficiency of 0.8 at the slots and decreasing linearly downstream at a rate of 0.05 per mm. At rows 'a' and 'g' the upstream adiabatic wall temperature is taken equal to 1500 K = 1227 °C and at row 'h' this is taken equal to the local film temperature behind row 'g'.

The FEM calculations are started with a uniform temperature of the blade material. After 15 minutes computation time on a work station and using 7 iteration steps, an accuracy of better than 1 degree C is obtained.

In figure 11 the resulting blade material temperatures are presented as well as the cooling flow temperatures at mid-span. Temperatures are given in degrees Celsius since this unit is very often used when materials properties are discussed.

It is noted that the air temperatures in the cooling ducts are higher than assumed when estimating the mass flows to evaluate the pressure loss in section 10.2. At orifice rows 'a' and 'g' the total temperature is 898 + 273 = 1171 K rather than 1050 K. This results in a 5.3 percent lower mass flow. This would require a second iteration cycle, not performed here.

The injection temperature is taken constant along the blade span and equal to the cooling air temperature at the end of the serpentine duct that feeds the orifices. The result is that the maximum temperature of the "blade segment" is found on the upper (suction) side near the end of the duct '3'. This temperature is slightly higher than the value at mid span.

The maximum material temperature is 989 °C in the case of orifice cooling with a local film cooling efficiency of 0.15. The mid-span value is 980 °C, see figure 11. The injection temperature for row 'a' is 923 °C and the resulting film temperature is 1181 °C.

In the case of slot cooling the maximum material temperature is 825 °C (a reduction of 164 °C) and 819 °C is found at mid span. Without adaptation, a CFD model representing orifice cooling by a slot cooling model will lead to unrealistic results for the present application.

Figure 12 shows the blade surface temperature distribution at mid-span according to fig.11 and the corresponding film temperature resulting from the assumed film cooling efficiencies. For both cooling methods the highest heat transfer is found at the downstream edge (points B and D). At point B a heat transfer of $345 \times 2.7 = 932$ kW/m^2 is found for the orifice cooling model and $318 \times 2.7 = 859$ kW/m^2 for the slot cooling model.

Temperature gradients in the blade material are of the order of 50 °C/mm and are maximum in the top wall of the first cooling duct where the temperature in the cooling ducts is low. If a flat plate is heated on one side such

that a temperature difference of 50 °C exists between the two sides and this plate is forced to remain planar, thermal stresses will develop. For a thermal expansion coefficient ε = 13 E-6 per deg C and a Youngs modulus E = 2.0 E+5 N/mm^2 a stress level is calculated of 65 / 0.7 = 93 N/mm^2. These material values are for a nickel alloy at room temperature. At higher temperatures E may be lower but this example illustrates that significant thermal stresses will exist that have to be analysed further and be related to creep and thermal fatigue, also taking into account the aerodynamic and centrifugal loads that occur.

10.4 Sensitivity to input data

The simple geometry model of figure 10 was used further to estimate the effect of variation of input data on the maximum blade temperature, using the orifice film cooling model and its results (Fig 11a and 12 left) as baseline. The following temperatures were found, changing one parameter as indicated while the others remain unchanged:

Temp in°C	Max wall temp	Max wall temp at mid span	Injection temp of row “a”	Film temp behind row “a”
Baseline	989	980	923	1181
1.25 h_{int}	975	965	901	1178
1.25 h_{ext}	1027	1018	954	1186
1.25 m_{cool}	962	953	877	1175
0.8 m_{cool}	1025	1017	968	1188
$\eta_{film} = 0.15 \rightarrow 0.25$	961	952	895	1144
$T_{cool,in} = 602 \rightarrow 677$	1019	1011	957	1187
$T_{gas} = 1227 \rightarrow 1377$	1083	1072	996	1320

The last row corresponds to an increase of the gas temperature by 10 percent from 1500 to 1650K (in the rotor frame of reference). This would correspond to a turbine entry temperature that is 10 percent higher than the (area) average value at the engine design point according to GSP. The resulting blade temperature in this case may indicate the value that would result from a temperature distortion in the radial direction with a peak temperature at mid span 10 percent above the area average value. The resulting value for the profile factor defined as $(T_{t4,max,rad} - T_{t4,avg})/(T_{t4,avg} - T_{t3})$ is 168 / (1675 – 821) = 0.197 (see also Ref. 8).

With this simulated temperature distortion a maximum materials temperature of 1083 °C results. This is close to the maximum short-time use temperature of the single crystal nickel alloys that are used in the F100-PW-220 engine.

The maximum (area average) turbine entry temperature that may occur during a flight mission is somewhat higher than the value of 1675 K (1402 °C) at the design point (sea level military thrust). On the other hand the film temperature at rows ‘a” and “g” will be lowered by the upstream orifice rows. This is not taken into account when calculating the film temperature behind these rows on the cooling block model of figure 10.

It is concluded that the present analysis provides a suitable method to calculate blade temperature histories sufficiently accurate to estimate engine blade life on a relative basis using the engine operational conditions as collected by the flight data recording system.

11. Conclusions

A method has been formulated to predict the temperature distribution in film cooled turbine blades. Input data are: the engine operational conditions and the geometry of the vanes and blades including the size and location of the film cooling orifices.

The input data are used as follows:

1. The Gas Turbine Simulation Program GSP translates the operational conditions in turbine entry and exit temperatures, pressures and mass flows including cooling air.
2. The distribution of the cooling air between the various blade rows is estimated from the orifice area and assumed cooling air pressures and temperatures inside the blades.
3. FINE/Turbo calculates the pressure and heat transfer coefficient distribution on the rotor blade without film cooling as well as the pressure distribution with film cooling using turbine entry and exit conditions from GSP. These heat transfer coefficients are also used for the situation with film cooling.

4. The internal heat transfer and pressure losses are estimated taking the values in fully developed turbulent pipe flows multiplied by factors to account for the presence of turbulators. These factors are typically 2 and 5 respectively.
5. The film cooling efficiency is a free variable and is typically 0.2 to 0.1 for orifice film cooling.

The following lessons have been learned:
1. CFD methods require very fine computational grids to realistically capture the flow and heat transfer near the film cooling injection orifices. At present this leads to computation times that are out-of-balance with an analysis that relates engine operational conditions during a flight mission to blade temperatures.
2. Modelling cooling orifices by means of a slot width of 1 to 5 percent of the blade chord can be used efficiently to calculate the effect of added mass by film cooling on the blade pressure distributions.
3. The value of film cooling efficiency is one of the most uncertain factors in the prediction of the blade temperatures when real blades with cooling orifices of optimised orientation are considered. The maximum materials temperature predicted with an orifice cooling efficiency of 0.15 is close to the maximum short-time use temperature of single crystal nickel alloys.
5. The present analysis provides a suitable method to calculate blade temperature histories sufficiently accurate to estimate engine blade life on a relative basis using the engine operational conditions as collected by the flight data recording system.

12. References

1. Colladay, R.S.; *Turbine Cooling*, Chapter 11 in: Turbine Design and Application, NASA SP-290 (1994).
2. Sellers, J.P.; *Gaseous Film Cooling with Multiple Injection Stations*, AIAA J. Sept. 1963, pp. 2154-2156.
3. Kadotani, K, and Goldstein, R.J.; *Effect of Mainstream Variables on Jets Issuing from a Row of Inclined Round Holes* J. Eng. for Power, April 1979, Vol. 101, pp 298-304.
4. Visser, W.P.J.; *GSP, A Generic Object-Oriented Gas Turbine Simulation Environment*, ASME-2000-GT-0002, NLR-TP-2000-267.
5. Gritsch, M., Schultz, A. and Wittig, S.; *Method for Correlating Discharge Coefficients of Film Cooling Holes, AIAA J Vol.36, No.6, June 1998, pp 976-980*).
6. Numeca International, FINE/Turbo User Manual (version 4.1), Numeca International, Brussels, April 2000.
7. Harasgama, S.P.; *Aerothermal Aspects in Gas Turbine Flows: Turbine Blade Internal Cooling*, VKI Lecture Series 1995-05.
8. Van Erp, C.A. and Richman, M.H.; *Technical Challenges Associated with the Development of Advanced Combustion Systems*, Paper 3 in RTO-MP-14, 1999.

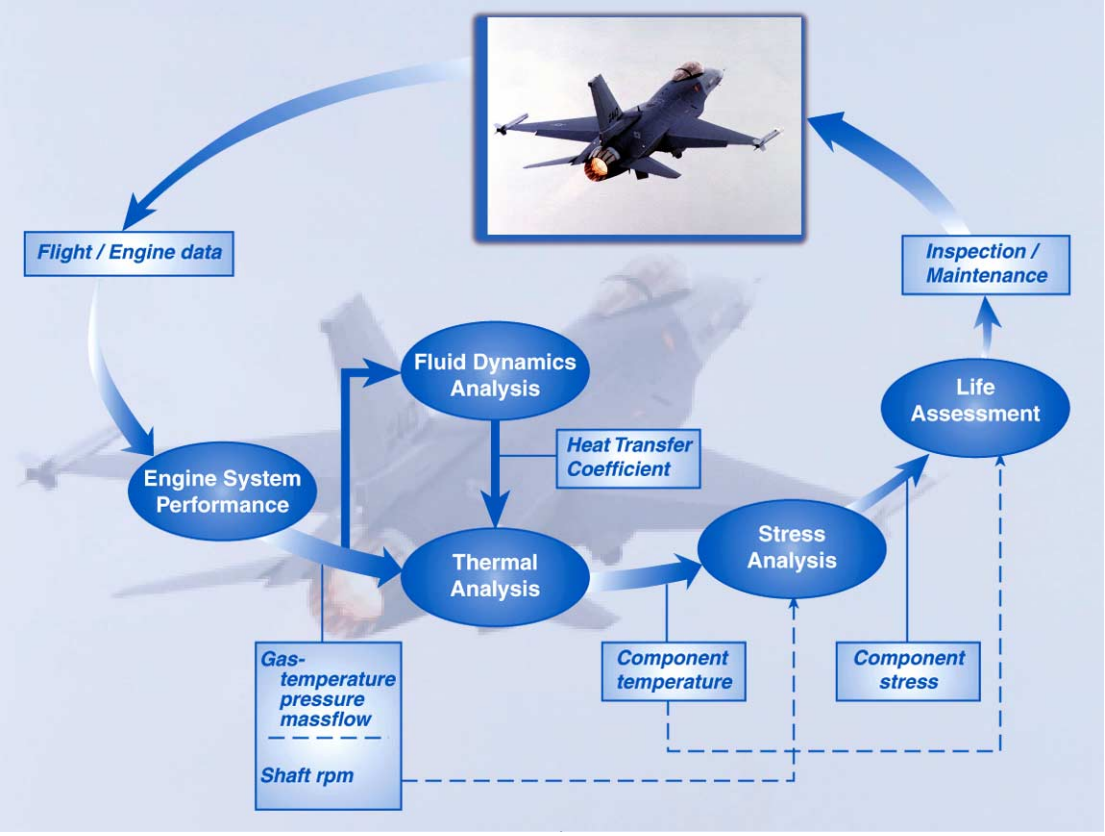

Fig. 1 Multi-disciplinary framework for life prediction model

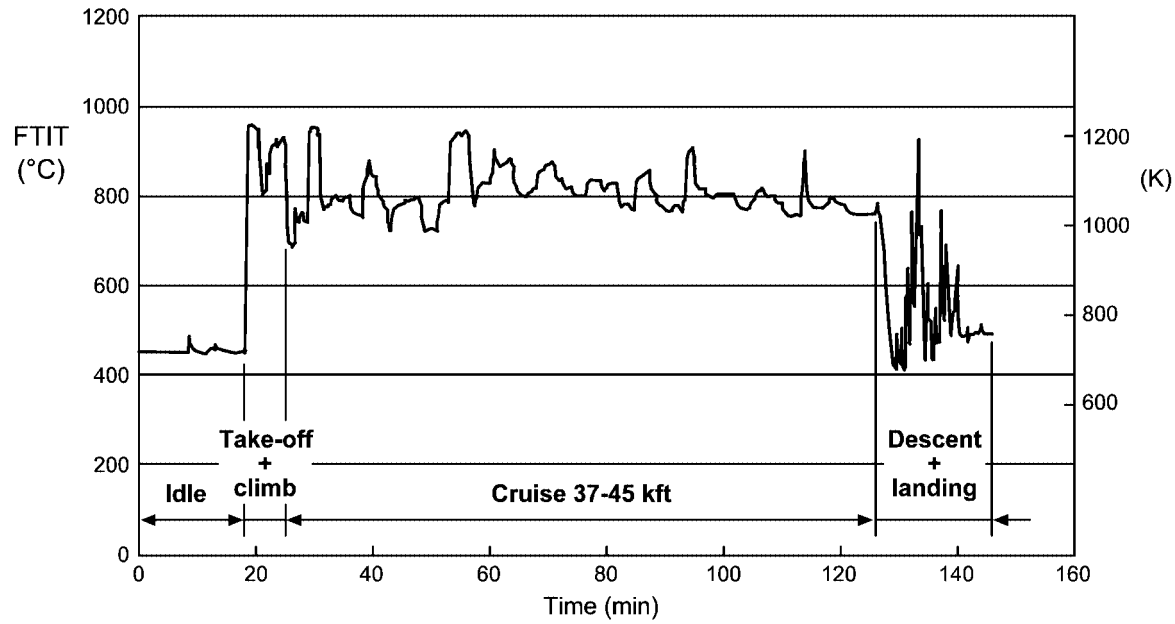

Fig. 2 HP turbine exit temperature variation of F-100-PW-220 turbofan engine recorded during an F-16 mission

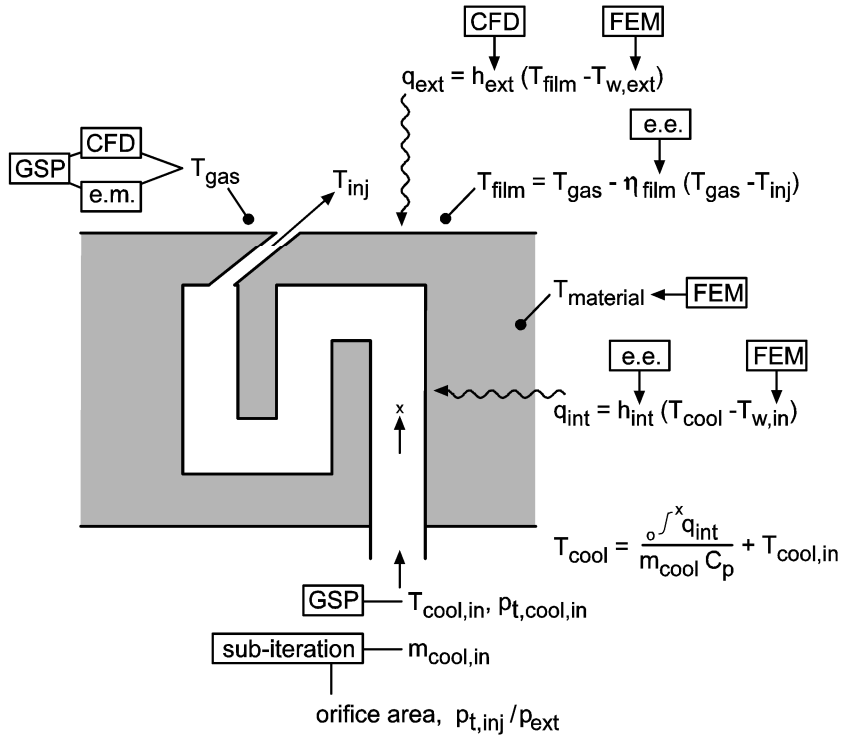

Fig. 3 Data flow logic in film cooling heat transfer calculations

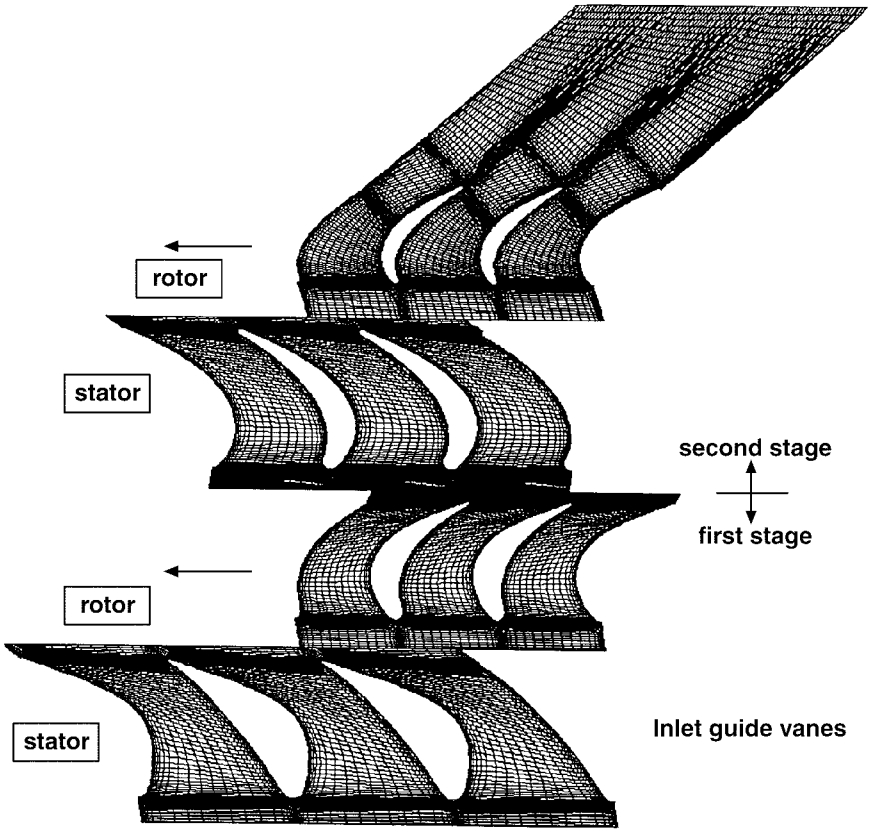

Fig. 4 F-100-PW-220 HP turbine blades at mid-span with grid used for CFD computations

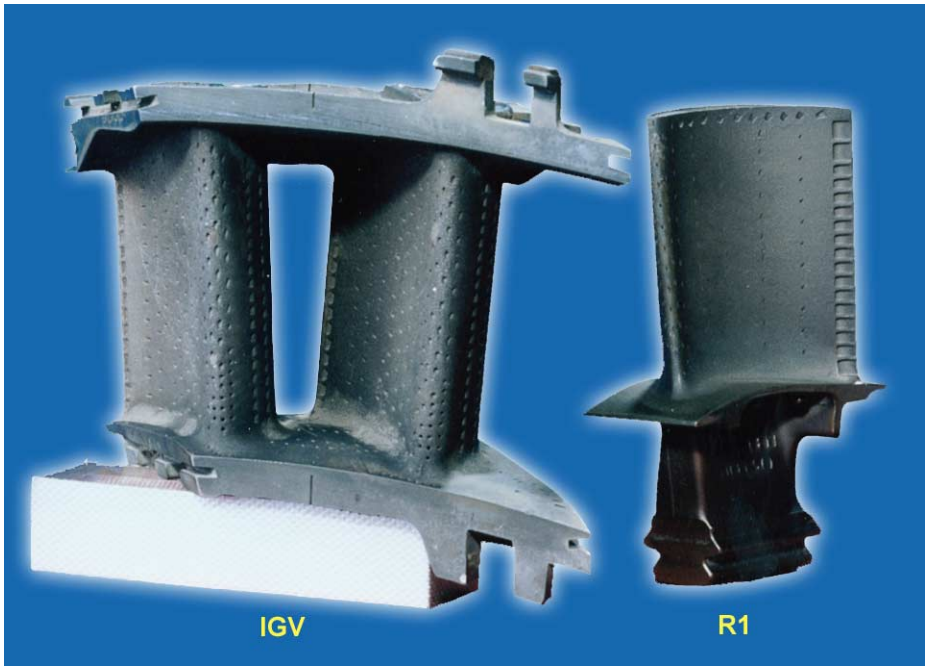

Fig. 5 F-100-PW-220 high-pressure turbine inlet guide vanes and first stage rotor blade

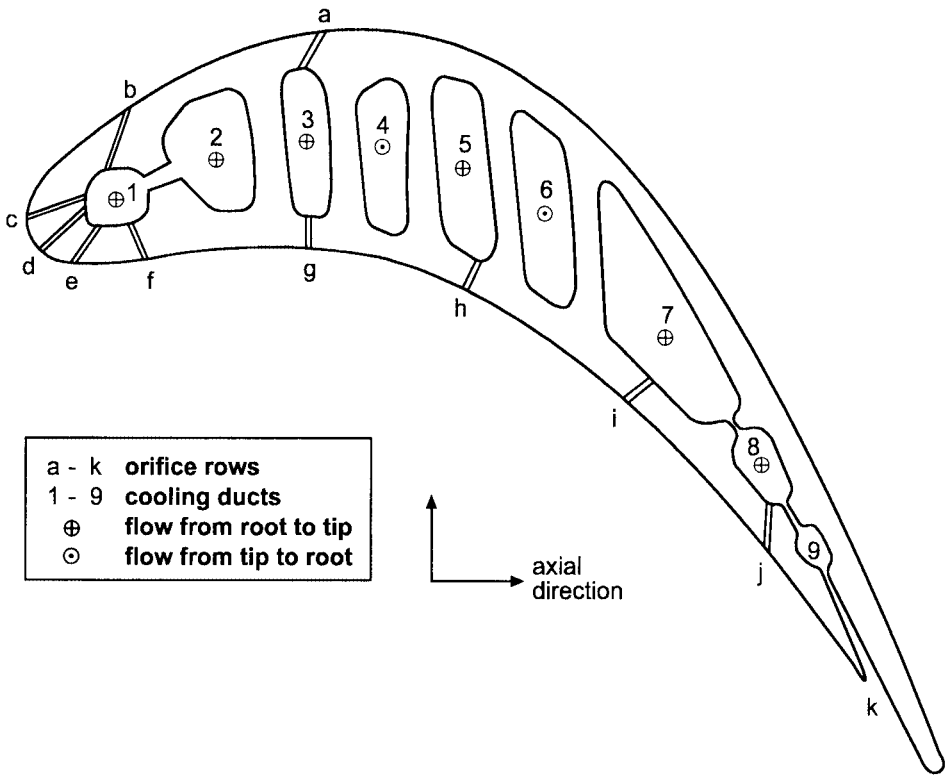

Fig. 6 First stage rotor blade with cooling ducts and film cooling orifices

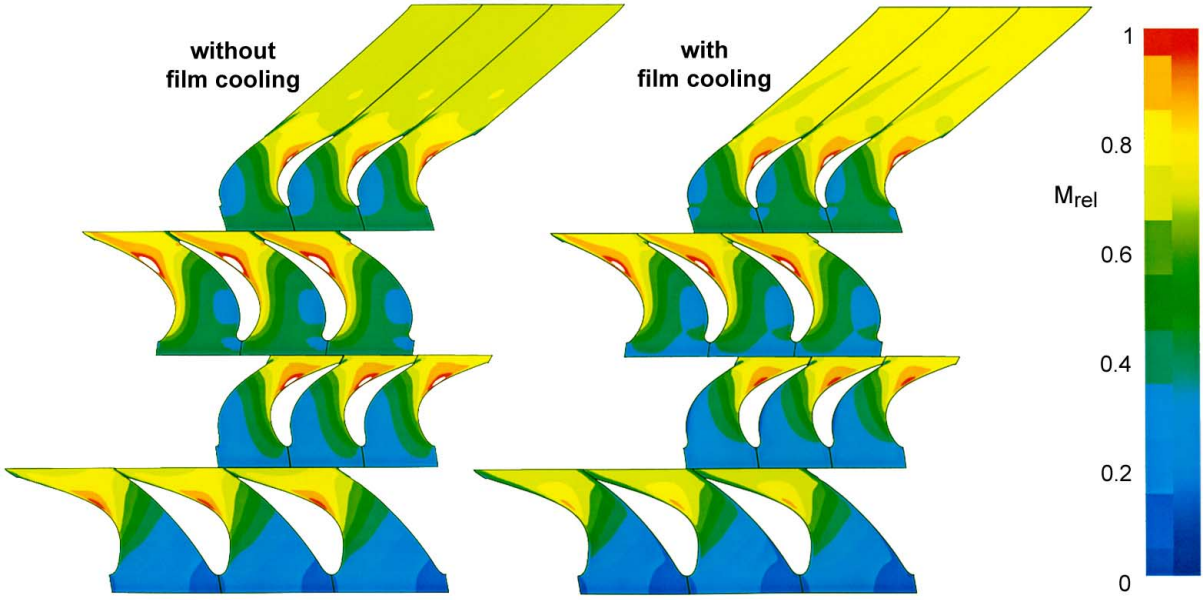

Fig. 7 Relative Mach numbers in HP-turbine at engine reference conditions

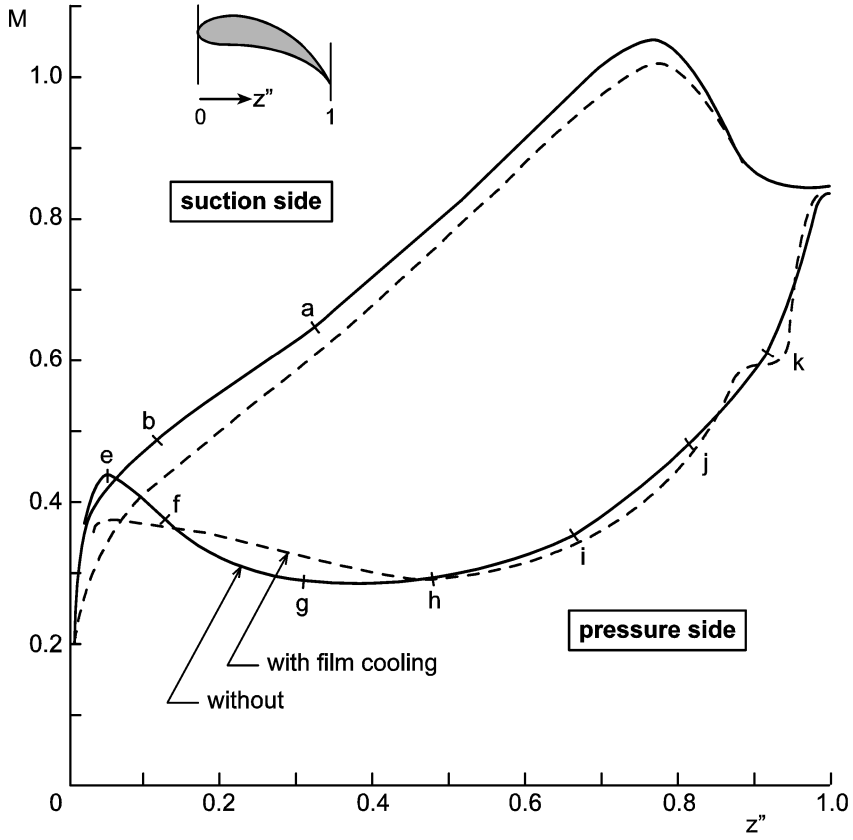

Fig. 8 Mach number on rotor blade outside the boundary layer as derived from surface pressure calculations

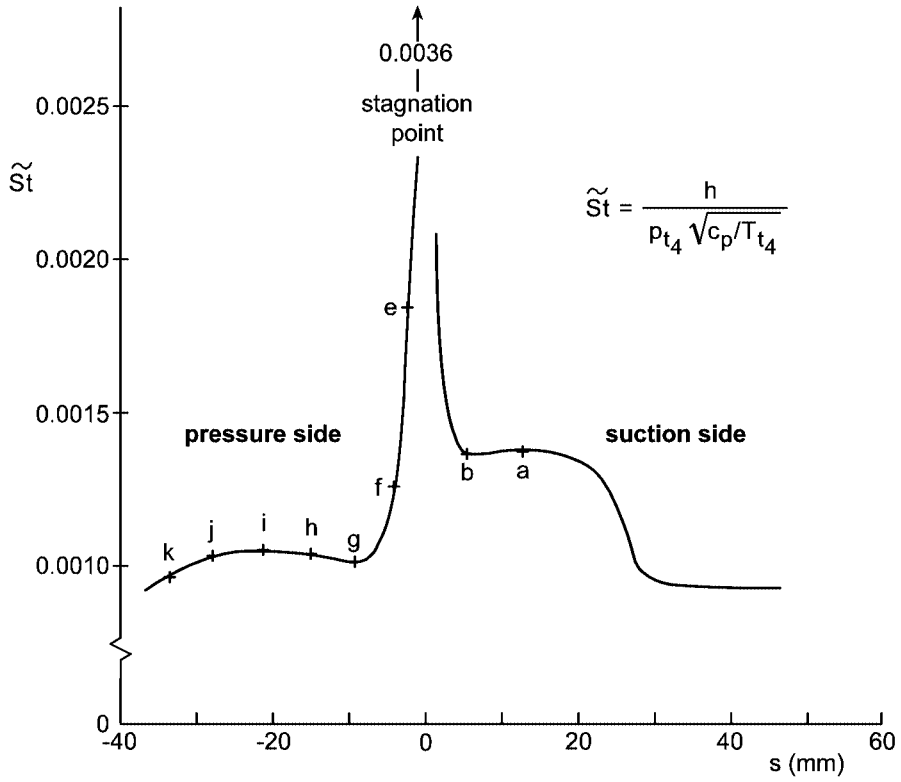

Fig. 9 Stantor number distribution on rotor blade at engine design point

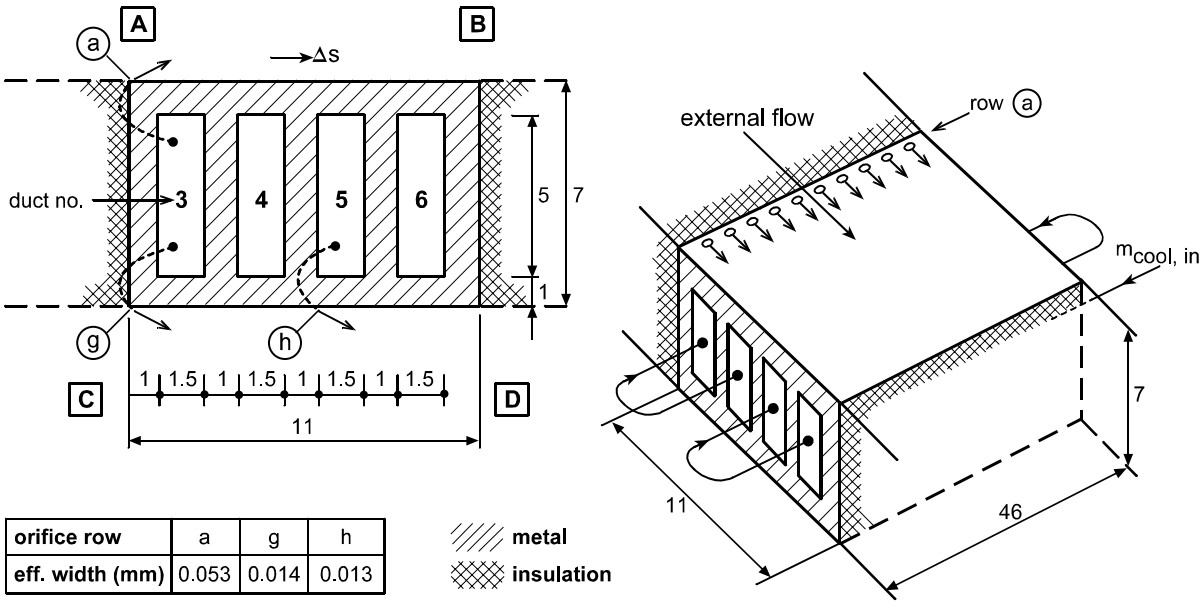

orifice row	a	g	h
eff. width (mm)	0.053	0.014	0.013

Fig. 10 Configuration to demonstrate coupled heat transfer analysis

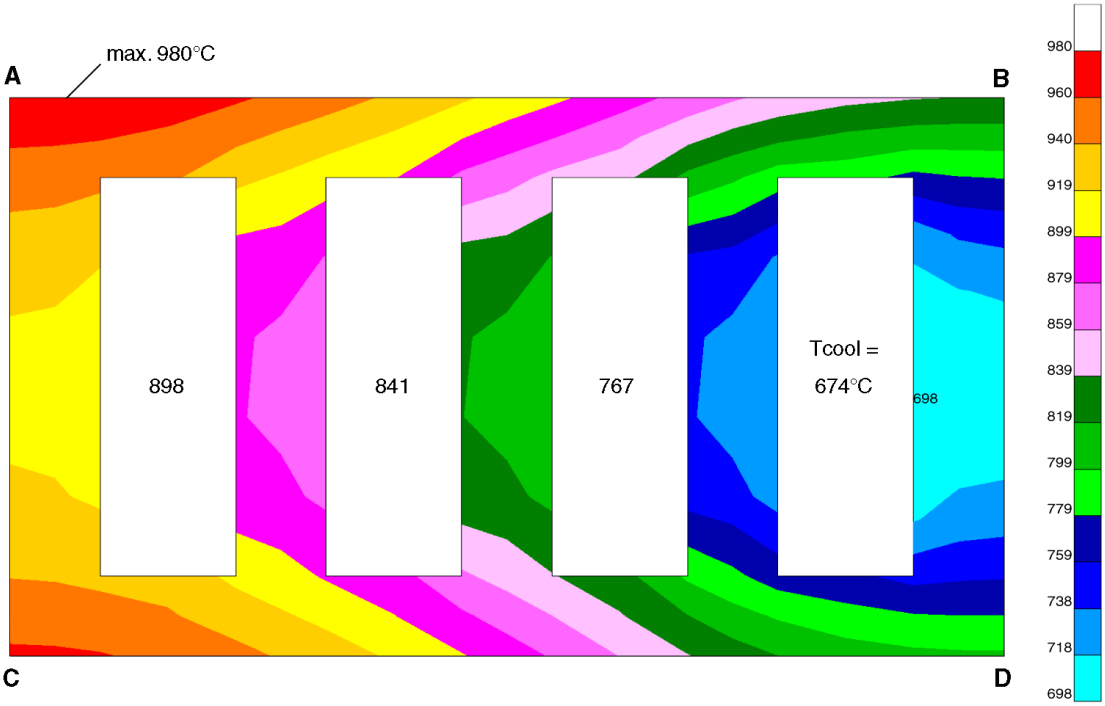

*Fig.11a Temperature distribution at midspan with **orifice cooling***

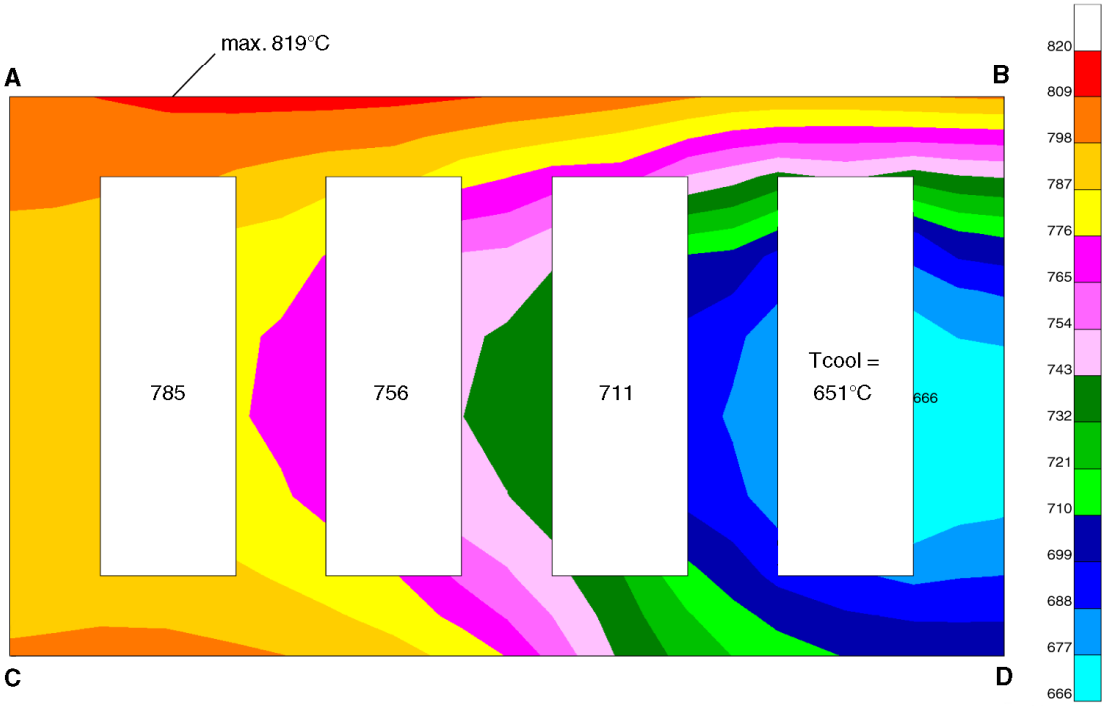

*Fig.11b Temperature distribution at midspan with **slot cooling***

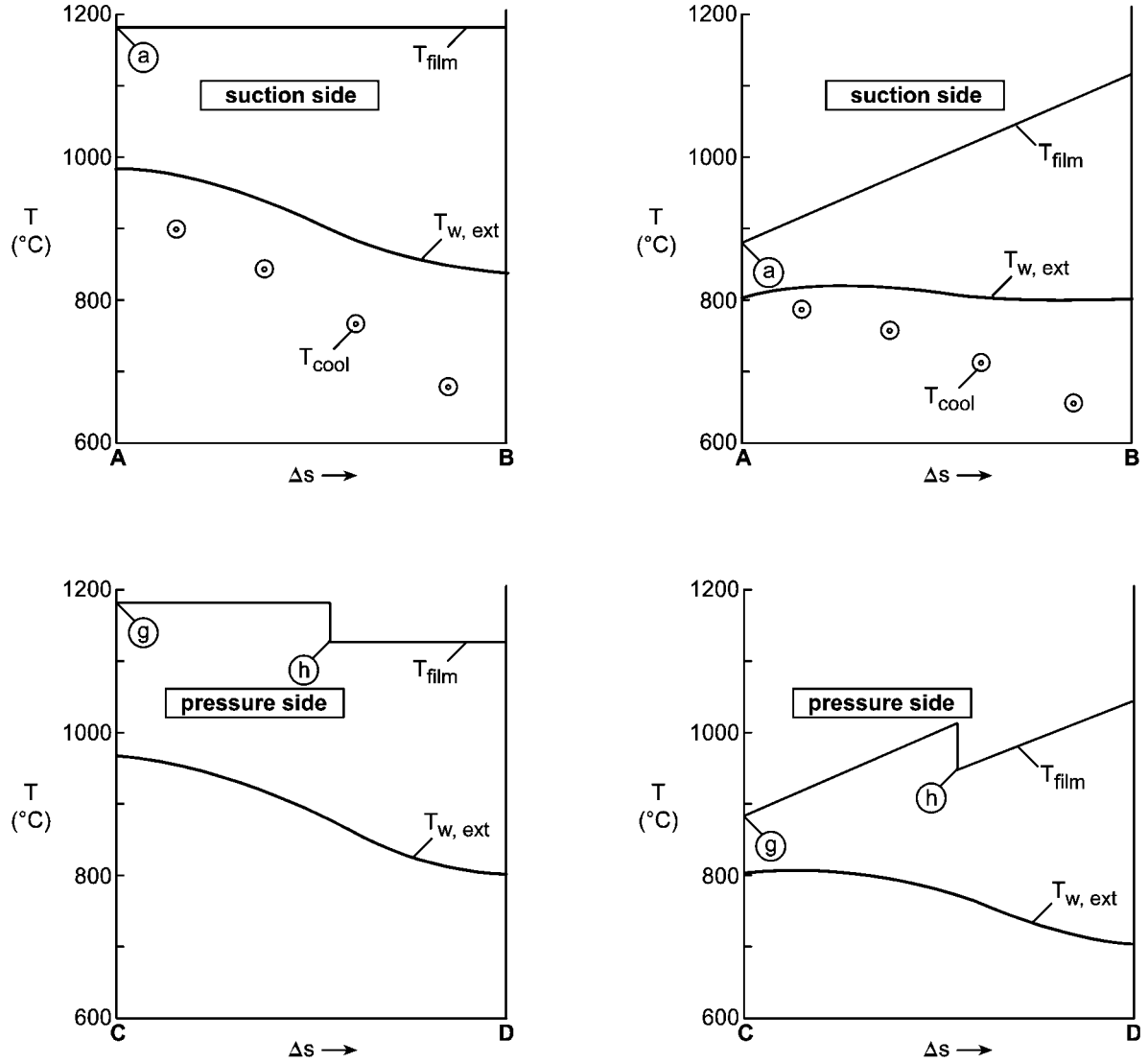

Fig. 12 Blade surface and film temperatures for orifice (left) and slot (right) cooling model

This page has been deliberately left blank

Page intentionnellement blanche